Revista Científica de Ingeniería, Industria y Arquitectura
Vol.9, Num.18 (jul-dec 2026) ISSN: 2737-6451

FINI BUS

Article

Determination of the Optimal Clay Nanoparticle Content in Mortars to Improve Compressive Strength Compared to Conventional Mortar for Plastering

Mohammadfarid Alvansazyazdi [1] **Diego Quimbia Tasgacho** [1] **Wilman Padilla Folleco** [1] **Karen Zambrano-Roldán** [2]

[1] Faculty of Engineering and Applied Sciences, School of Civil Engineering, Central University of Ecuador. Quito, Ecuador.

[2] Faculty of Engineering, Industrial and Architecture, School of Civil Engineering, Laica Eloy Alfaro de Manabí University, Manta, Ecuador.

Corresponding author: farid.alvan@uce.edu.ec

Abstract

This study focuses on enhancing the mechanical properties of plaster mortars through the incorporation of clay nanoparticles. The main objective was to determine the optimal dosage of clay nanoparticles by evaluating their effect on compressive strength, water absorption, and permeability, supported by nanometric-scale microstructural analysis. Mortars were prepared using Holcim type N cement and Selvalegre type HS cement, local washed quarry sand, and potable water. Clay nanoparticles were added at 0.25%, 0.50%, 0.75%, and 1.00% replacing part of the cement. The mortars underwent characterization tests including fine aggregate analysis, compressive strength, absorption, permeability (contact angle), and microstructural evaluations using SEM, TEM, XRD, and EDS. All tests were conducted under controlled temperature and humidity following national standards (NTE INEN 488, 2518, 2536) and applicable ASTM norms. Results showed that a 0.25% nanoparticle dosage was most effective, increasing compressive strength from 12.60 to 16.61 MPa in type N mortars and from 30.54 to 37.87 MPa in type HS mortars. Water absorption slightly decreased in type N and slightly increased in type HS mortars. Permeability analysis revealed hydrophilic behavior in type N mortars and a shift from hydrophobic to hydrophilic in type HS mortars. Microstructural analysis indicated a denser matrix and enhanced chemical and physical interactions between nanoparticles and hydration products, improving durability and mechanical performance. It is concluded that 0.25% clay nanoparticles is the optimal dosage to significantly improve mechanical properties without negatively affecting absorption and permeability. This improvement is applicable for mortars used in plastering works requiring enhanced strength. However, nanoparticle incorporation increases costs by 63.26% compared to conventional mortars, requiring prior cost-benefit analysis for practical application.

Keywords: *clay nanoparticles; plaster mortar; compressive strength; optimal dosage; mechanical properties.*

Artículo original

Determinación del contenido óptimo de nanopartículas de arcilla en morteros para mejorar la resistencia a la compresión en comparación con el mortero convencional para enlucido

Resumen

Este estudio se centra en mejorar las propiedades mecánicas de los morteros de yeso mediante la incorporación de nanopartículas de arcilla. El objetivo principal fue determinar la dosificación óptima de nanopartículas de arcilla evaluando su efecto sobre la resistencia a la compresión, la absorción de agua y la permeabilidad, con el apoyo de un análisis microestructural a escala nanométrica. Los morteros se prepararon utilizando cemento Holcim tipo N y cemento Selvalegre tipo HS, arena de cantera lavada local y agua potable. Se añadieron nanopartículas de arcilla en proporciones de 0,25 %, 0,50 %, 0,75 % y 1,00 %, sustituyendo parte del cemento. Los morteros se sometieron a ensayos de caracterización que incluyeron análisis de agregados finos, resistencia a la compresión, absorción, permeabilidad (ángulo de contacto) y evaluaciones microestructurales mediante SEM, TEM, XRD y EDS. Todos los ensayos se realizaron bajo temperatura y humedad controladas, siguiendo las normas nacionales (NTE INEN 488, 2518, 2536) y las normas ASTM aplicables. Los resultados mostraron que una dosificación de nanopartículas del 0,25 % fue la más efectiva, aumentando la resistencia a la compresión de 12,60 a 16,61 MPa en morteros tipo N y de 30,54 a 37,87 MPa en morteros tipo HS. La absorción de agua disminuyó ligeramente en los morteros tipo N y aumentó ligeramente en los morteros tipo HS. El análisis de permeabilidad reveló un comportamiento hidrofílico en los morteros tipo N y un cambio de hidrofóbico a hidrofílico en los morteros tipo HS. El análisis microestructural indicó una matriz más densa y una mayor interacción química y física entre las nanopartículas y los productos de hidratación, lo que mejora la durabilidad y el rendimiento mecánico. Se concluye que el 0,25 % de nanopartículas de arcilla es la dosificación óptima para mejorar significativamente las propiedades mecánicas sin afectar negativamente la absorción y la permeabilidad. Esta mejora es aplicable a morteros utilizados en trabajos de enlucido que requieren mayor resistencia. Sin embargo, la incorporación de nanopartículas aumenta los costos en un 63,26 % en comparación con los morteros convencionales, lo que requiere un análisis previo de costo-beneficio para su aplicación práctica.

Palabras Clave: *nanopartículas de arcilla; mortero de yeso; resistencia a la compresión; dosificación óptima; propiedades mecánicas.*

Suggested citation: Alvansazyazdi, M.; Quimbia Tasgacho, D., Padilla Folleco, W., & Zambrano-Roldán, K. (2026). Determination of the Optimal Clay Nanoparticle Content in Mortars to Improve Compressive Strength Compared to Conventional Mortar for Plastering. *Revista Científica FINIBUS – Ingeniería, Industria y Arquitectura.* 9(18) 115-134 https://doi.org/10.56124/finibus.v9i18.010

DOI: https://doi.org/10.56124/finibus.v9i18.010

Received: 15-09-2025 *Review: 05-01-2026*
Accepted: 02-02-2026 *Published: 01-07-2026*

1. Introduction

This research aims to develop an innovative mortar with enhanced strength properties, while also evaluating adjacent physical characteristics such as absorption, permeability, and nanometric characterization to support the results obtained (Alvansazyazdi et al., 2019). This approach could represent a significant step toward the creation of more sustainable and high-performance construction materials (Alvansazyazdi et al., 2025a). Nanotechnology has long been a reality in various fields of daily life; however, its limited applications in the construction industry have not yet been consolidated (Golshan et al., 2012). This is largely due to strategies that rely on combining expensive nanomaterials with conventional cementitious materials. Although such practices may produce some positive effects on material properties, they also significantly reduce the primary competitive advantage of cement-based materials: their low cost. Therefore, this study proposes and successfully tests a new approach (Alvansaz Yazdi et al., 2014; Gaitero Redondo, 2011).

Among the documented advances, pozzolanic nanoparticles such as nanosilica have been shown to increase strength and reduce porosity; titanium dioxide (TiO_2) contributes environmental benefits through contaminant reduction; and nanometric-scale void filling generates denser microstructures with lower free water content (Alvansazyazdi et al., 2025b, 2025c; López Molina, 2013). Previous studies have demonstrated that modified clays can act as pozzolanic or nucleating agents, accelerating hydration and improving mortar compactness, thereby supporting their use in the development of more efficient and sustainable cementitious composites (Alvansazyazdi & Rosero, 2019; Guzmán Cardona et al., 2024). Several investigations have shown that the incorporation of nanoparticles in mortars significantly improves compressive strength and other physicomechanical properties compared to conventional mortars. The best results have been achieved with 2% nanosilica, 2–4% nanoalumina, and the combination of 3% nanosilica with 1% nanoalumina, the latter reaching the highest strength (Alvansaz et al., 2022; Andrade Vieira, 2017).

Nanotechnology applied to mortars and concretes is transforming the way hydraulic mixtures are designed, since even small doses of nanoparticles can substantially alter the physicochemical properties of the base material (Franco-Luján et al., 2023). Due to their reduced size and high surface-to-volume ratio, these particles enhance matrix density, accelerate hydration, and act as nucleating agents that promote the formation of C-S-H gel (Abhilash et al., 2021; Franco-Luján et al., 2023). Recent studies on nanoclay (montmorillonite) indicate that dosages below 3% of the cement significantly improve mechanical strength and reduce permeability, thanks to its function as a fine filler and hydration catalyst. This contributes to densifying the microstructure and reducing water absorption (Bunea et al., 2023; Kafi et al., 2016). Future perspectives point toward the engineering of materials specifically designed for each application, supported by advanced techniques in synthesis, characterization, and computational modeling (Franco-Luján et al., 2023).

To study the properties of cementitious materials at the nanoscale, analytical techniques such as X-ray Diffraction (XRD), Scanning Electron Microscopy (SEM), Energy Dispersive X-ray Spectroscopy (EDS), and Transmission Electron Microscopy (TEM) are used. These methods enable the understanding of phase variations in cement and cementitious systems during hydration in the presence of nanomaterials (Alvansazyazdi et al., 2025d; Ray et al., 2021).

This study is presented as an experimental contribution aimed at establishing the optimal proportion of nanoclay in mortar mixtures, evaluating their mechanical performance over time under controlled conditions. Identifying the optimal addition percentage, analyzing its effects on microstructure, and assessing potential technical and economic advantages guide the methodology, allowing for a critical comparison of the performance of modified mortar against conventional mortar. It is hypothesized that the incorporation of clay nanoparticles significantly enhances mortar performance for plastering applications, by increasing compressive strength, reducing absorption and permeability, and reinforcing internal cohesion, thereby contributing to durability. Furthermore, the modified mortar is expected to offer additional properties such as greater impermeability and potential improvement in acoustic insulation. The findings will be valuable for professionals and industries seeking to optimize their products without increasing costs or compromising sustainability (Alvansaz et al., 2019; Alvansazyazdi et al., 2024a).

2. Materials and Methods

2.1 Materials used

In this study, two types of cement (Table 1) were employed for the preparation of mortars. “Holcim Maestro” Type N cement is designed for high-quality masonry work and provides a 50% reduction in CO_2 emissions, meeting and exceeding the requirements of the NTE INEN 1806 standard for non-structural use cements (Alvansazyazdi et al., 2025e; Holcim, 2022). Meanwhile, “Selvalegre Campeón” Type HS cement is a hydraulic cement with high sulfate resistance, intended for dense concretes and structures requiring durability against aggressive soils and waters, in compliance with the NTE INEN 2380 standard (Alvansazyazdi et al., 2025f; Cemento Selvalegre, 2025). The density of the cement used was determined in the laboratory prior to mortar preparation, following the NTE INEN 156:2009 standard. The values obtained were 2.82 g/cm³ for Type N and 2.836 g/cm³ for Type HS, both of which comply with the standards required for proper performance in cementitious mixtures.

Table 1. Density type N and type HS cement

Test	**Cement Density**	
Cement	Maestro Holcim	Campeón Selvalegre
Type	N	HS
#1 (g/cm³)	2.83	2.83
#2 (g/cm³)	2.82	2.83
#3 (g/cm³)	2.81	2.85
Average (g/cm³)	2.82	2.836

The fine aggregate used was washed natural sand from the Copeto quarry (Santo Domingo de los Tsáchilas), selected in accordance with ASTM C33. This sand meets the requirement of 100% passing through the No. 3/8” sieve, is free of impurities, and exhibits controlled gradation, ensuring proper workability and compaction of the mortar (Table 2, Figure 1) (ASTM International, 2018; Morales et al., 2020). Characterization of the fine aggregate was carried out following various Ecuadorian standards. Gradation was evaluated according to NTE INEN 696:2011 (Instituto Ecuatoriano de Normalización [INEN], 2011a), obtaining an average fineness modulus of 2.48 from three samples, within the optimal range of 2.3–3.1.

Table 1. Sieve Analysis of Fine Aggregate – Sample 3

FINE AGGREGATE – SAMPLE No. 3 - Po=500,4 g					
Sieve	**Retained**		**% Retained**	**% Passing**	**Specification Limits**
	Partial (g)	**Cum. (g)**			
3/8	0,00	0,00	0,00	100,00	100
N.°4	**0,00**	**0,00**	**0,00**	**100,00**	**95 - 100**
N.°8	6,60	6,60	1,32	98,68	80 - 100
N.°16	**99,90**	**106,50**	**21,32**	**78,68**	**50 - 85**
N.°30	149,20	255,70	51,19	48,81	25 - 60
N.°50	**145,40**	**401,10**	**80,30**	**19,70**	**10 - 30**
N.°100	76,70	477,80	95,66	4,34	2 - 10
N.°200	**14,60**	**492,40**	**98,58**	**1,42**	**0 - 2**
Pan	7,10	499,50	100,00	0,00	
∑	**499,50**				
Mo (g)	500,40	0,90			
% Error (< 0.3)	**0,9982**	**0,18%**	**MF (2.3-3.1) =**		**2,50**

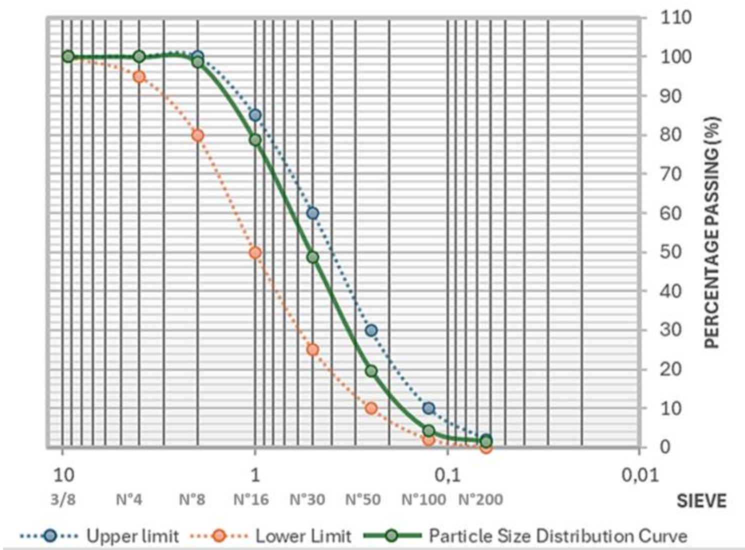

Figure 1. Grain Size Distribution Curve of Fine Aggregate – Sample 3.

The content of fine material passing through the No. 200 sieve was determined according to NTE INEN 697:2010 (INEN, 2010a), resulting in 1.9%, below the maximum limit of 3%. Density, specific gravity, and absorption were measured following NTE INEN 856:2010 (INEN, 2010b), yielding values of 2.74 g/cm³ and 1.7%, respectively, within the accepted ranges. The loose and compacted unit mass was evaluated according to NTE INEN 858:2010 (INEN, 2010c), with results of 1573 kg/m³ and 1695 kg/m³, respectively, falling within reference ranges. The presence of organic impurities was analyzed according to NTE INEN 855 (INEN, 2010d), showing no significant content; friable particles were determined following NTE INEN 698 (0.8–1.2%) (INEN, 2010e) and lightweight particles according to NTE INEN 699 (0.4%) (INEN, 2011b), both below the maximum allowable limits. All results confirm that the fine aggregate meets the required standards to produce high-quality mortars (Table 3).

Table 2. Summary of Fine Aggregate Characterization

General Characterization of Fine Aggregate			
Test	Value	Unit	Range
Fine material, passing °200 sieve	1.9	%	<3%
Density	2.74	g/cm³	2.5-2.8 g/cm³
Absorption	1.7	%	<3%
Loose unit weight	1573	kg/m³	1200–1750 kg/m³
Compact unit weight	1695	kg/m³	1400–1900 kg/m³
Colorimetry 	Gardner 1 White to Transparent	Escala de Gardner	 Gardner >5
Friable Particles	0.8-1.2	%	<2%
Light Particles	0.4	%	<1%

Potable water was used in compliance with the specifications of ASTM C1602/C1602M, which regulates mixing water for concrete and mortar (ASTM International, 2022). The Nanoclay (Figure 2), surface-modified, containing 25–30 wt.% trimethyl stearyl ammonium, supplied by Sigma-Aldrich, was employed, specifically designed to disperse effectively within cementitious matrices (Alvansazyazdi et al., 2025g, 2025h). Although the aggregates may measure up to < 20 µm, the individual platelets exhibit nanometric dimensions, with particle sizes below 100 nm (Alvansazyazdi et al., 2025i; Sigma-Aldrich, 2011).

Figure 2. Specifications of the Used Nanoclay.

2.2. Standard Mixing Procedure, Modified Mixture, and Tests

The study methodology is presented through a flowchart detailing the fundamental stages (Figure 3), all supported by a thorough review of relevant standards: material characterization, experimental design, test execution, and interpretation of results (Alvansazyazdi et al., 2024b). This framework ensures clarity, standardization, and replicability of the process, thereby guaranteeing scientific rigor in accordance with current regulations, as developed in this section. To this end, a comparative experiment was designed with one control group and several experimental groups, while keeping all other parameters that may influence the material's strength constant (Alvansazyazdi et al., 2024c, 2024d; Hernández Sampieri et al., 2014).

In section A of this chapter, the description and characterization of the materials used were established. The following presents a brief explanation of the reference mix proportion. According to the Ecuadorian Technical Standard NTE INEN 488:2009, which specifies the test method for determining the compressive strength of mortars in 50 mm cube specimens, each mortar batch must be prepared with three specimens for each testing age. For this research, a standard mix proportion of 740 g of cement and 2,035 g of sand was used, adjusting the amount of water required to achieve a flow of 115% on the flow table, thus meeting the requirements of the standard, which specifies a flow range of 110 ± 5% in 25 drops, as detailed in NTE INEN 2500 (Alvansazyazdi et al., 2025j; INEN, 2009a). The specimens were tested at 1, 3, and 7 days to evaluate compressive strength. The maximum permissible range of variation among the three specimens is 9.4%. If the variation exceeds this limit, the value furthest from the average is discarded, and the range of the remaining two specimens is verified. If fewer than two valid values remain after this procedure, the test must be repeated (Table 4) (Alvansazyazdi et al., 2023; INEN, 2009b).

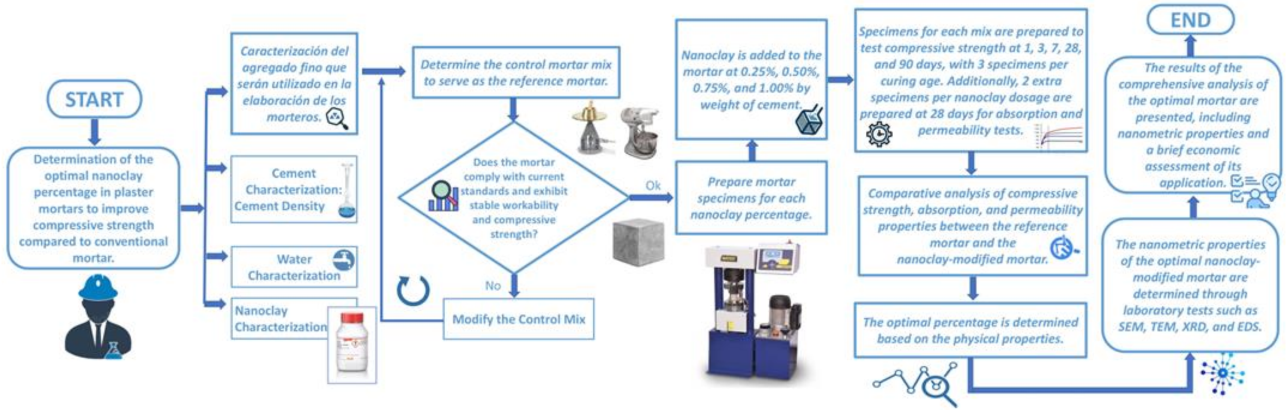

Figure 3. Flowchart of the Methodology Used in the Study.

Table 3. Mix proportion, w/c ratio, and flow of the reference mortars obtained

Number of Specimens	9 Mortar Cubes	
Material	Type N	Type HS
Cement (g)	740	740
Sand (g)	2035	2035
Water (cm3)	423.1	412.2
RETIO W/C	0.572	0.557
FLOW (%)	115	114

Since the specimens of the reference mix were found within this margin of error, it can be concluded that the mix proportion is stable and reproducible. Therefore, it can be used as a reference for the modified mixes with nanoclay at 0.25%, 0.50%, 0.75%, and 1.00% (three specimens per dosage tested at 1, 3, 7, 28, and 90 days; testing ages). This procedure ensures that the specimens meet the criteria for workability, uniformity, and reliability of compressive strength as established by the standard (Table 5).

Table 4. Material Quantities for Mortars According to Nanoclay Percentage

% Nanoclay	0,25%	0,50%	0,75%	1,00%
Ages	1 – 3 – 7 – 28 – 90 días			
Material	Material Quantity (g)			
Type N Cement				
Cement	738,15	736,3	734,45	732,6
Sand	2035	2035	2035	2035
Water	423,1	423,1	423,1	423,1
Nanoclay	1,85	3,7	5,55	7,4
Type HS Cement				
Cement	738,15	736,3	734,45	732,6
Sand	2035	2035	2035	2035
Water	412,2	412,2	412,2	412,2
Nanoclay	1,85	3,7	5,55	7,4

2.2.1. Mortar preparation

Cracking and drying were carried out to obtain a representative sample free of surface moisture, ensuring the accuracy of the tests. Cracking allowed the aggregate to be divided systematically and homogeneously, while oven dries at a controlled temperature until constant mass, following the standard, ensured the elimination of moisture. This procedure guarantees that the sample is statistically representative of the original batch and validates laboratory results (Alvansazyazdi et al., 2025k; INEN, 2009b). The nanoclay was previously dispersed in water by mechanical stirring at 888.9 RPM, to ensure homogeneous distribution and prevent agglomeration. This pre-mixing promotes proper interaction of the nanomaterial with the cementitious matrix and optimizes its effect on the properties of hardened mortar. Cement, sand, nanoclay, and water were accurately dosed using a calibrated electronic balance, ensuring precise mix proportions and guaranteeing reproducibility and reliability of the experimental results.

The mixing process consisted of an initial homogenization of cement and water for 30 seconds, followed by the incorporation of sand and, in nanoclay mixtures, the pre-dispersed additive, continuing with another 30 seconds of mixing. Subsequently, a 90-second pause was performed to reincorporate material adhered to the walls and bottom of the container, preventing losses or segregation. Finally, mixing was resumed for 60 additional seconds, completing an effective mixing time of 3 minutes, according to the standard (INEN, 2009b).

The workability of fresh mortar was evaluated using the flow table test established by ASTM C1437, which involves placing the mixture in a truncated cone mold, removing it, and applying 25 jolts in 15 seconds, then measuring the average spread diameter. This parameter reflects mortar workability and depends on factors such as water–cement ratio, particle size distribution, and the presence of additives. Values of 110–115 mm correspond to standard mortars, whereas higher spreads indicate greater fluidity with segregation risk, and lower values indicate drier, less workable mixes (ASTM International, 2020a; Neville, 2011). Cubic specimens of 5 × 5 × 5 cm were molded according to ASTM C109/C109M in two manually compacted layers. After 24 hours, the specimens were demolded and cured in water at 20 ± 2 °C until testing at 1, 3, 7, 28, and 90 days (INEN, 2009b; Salgado et al., 2019).

2.2.2. Compressive Strength Test

Compressive strength was determined by testing at least three specimens per condition, using a calibrated hydraulic press that applied continuous axial load until failure, in accordance with ASTM C109/C109M-20b. The maximum recorded load was converted to compressive stress (MPa), allowing evaluation and comparison of the mechanical performance of nanoclay-modified mortars with conventional mortars (ASTM International, 2020b; INEN, 2009b).

2.2.3. Water Absorption Test

Water absorption, related to mortar porosity and durability, was determined according to ASTM C642-13, adapted for 5 × 5 × 5 cm cubes. The samples were oven-dried at 105 ± 5 °C until constant mass (m_1), weighing every 2 hours to verify stability and extending drying time, if necessary, until confirming the driest condition. Subsequently, the specimens were immersed in water for 24 hours, and periodic weighing's were performed until saturated mass (m_2) stabilized. The absorption percentage was calculated from the difference between these two masses, allowing evaluation of the material's response to moisture and external agents (ASTM International, 2013).

2.2.4. Permeability Test

The contact angle test, regulated by ASTM D7334-08, was used as an indirect method to evaluate the surface permeability of the mortar. It consists of measuring the angle formed by a water droplet on the specimen surface, determining whether it is hydrophilic (<90°) or hydrophobic (>90°), and thus its tendency to absorb or repel moisture. The procedure was carried out using samples with uniform surfaces, controlled droplet volumes, and optical analysis with a goniometer and specialized software under stable environmental conditions. This test allowed comparison between conventional mortars and nanoclay-modified mortars to determine the additive's effect on water penetration resistance and material durability (Figure 4) (ASTM International, 2008).

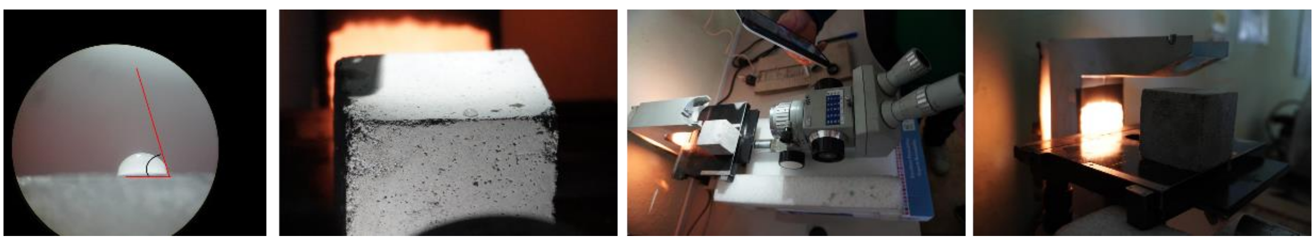

Figure 4. Contact Angle Measurement Process – Surface Permeability Assessment.

3. Results

3.1 Properties in Fresh State

The flow test, performed in accordance with NTE INEN 2500:2014 (Servicio Ecuatoriano de Normalización, 2014) and ASTM C1437 (ASTM International, 2020b), showed that the incorporation of nanoclay causes a progressive decrease in workability in both types of cement (N and HS), with the addition of nanoclay being indirectly proportional to the fluidity of the mortar but still remaining within the recommended range for plaster mortars (105–115%).

3.1.1. Type N Cement

The standard mortar had a fluidity of 116%, while the addition of nanoclay caused a progressive reduction, reaching 106% with 1.00% nanoclay. The dosages of 0.25% and 0.50% maintained workability within the recommended upper range (113% and 109%, respectively), ensuring good handling on site. The variation in mortar fluidity according to the percentage of nanoclay is shown in Figure 5.

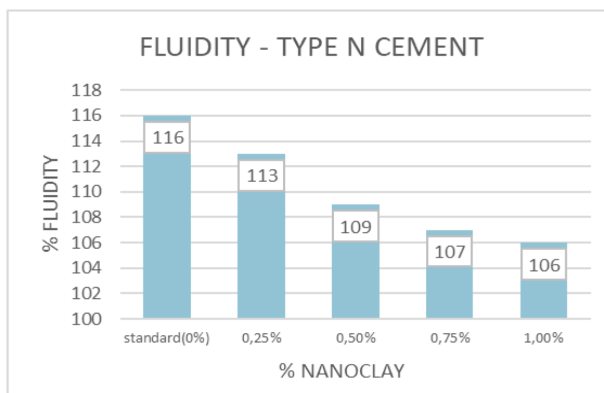

Figure 5. Variation in mortar fluidity with type N cement, depending on the addition of nano-clay

3.1.2. Type HS Cement

The fluidity of the standard mortar was 114%, decreasing to 108% with 1.00% nanoclay. The best ratio between workability and stability was achieved with 0.25% nanoclay (113%), while consistency was more affected at dosages of 0.50% and above. These results are shown in Figure 6.

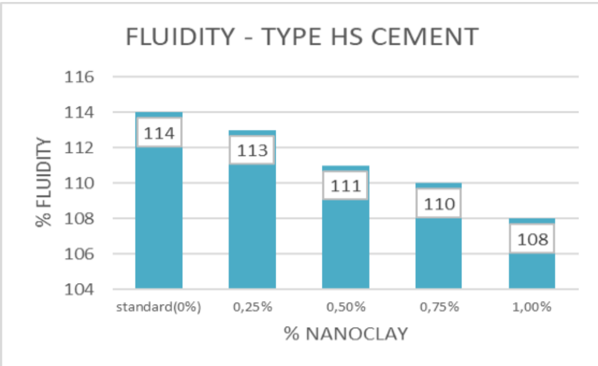

Figure 6. Variation in mortar fluidity with HS cement, depending on the addition of nano-clay

3.2. Compressive Strength

The evolution of strength, evaluated at 1, 3, 7, 28, and 90 days, showed similar behavior in both cements (Type N and Type HS), with a significant increase with 0.25% nanoclay and stabilization or reduction at higher doses.

3.2.1. Type N Cement

At 90 days, the standard reached 12.60 MPa, while with 0.25% nanoclay, 16.61 MPa (+31.8%) was achieved. Higher doses did not show consistent improvement: 0.50% → 12.94 MPa; 0.75% → 13.16 MPa; and 1.00% → 13.81 MPa. The maximum yield was obtained at 0.25%, with evident increases also at 28 days. The compressive strength results over time are presented in Table 6, while their graphical behavior is shown in Figure 7.

3.3. Absorption

Water absorption was evaluated in mortars with Type N and Type HS cements, incorporating nanoclay in proportions of 0.25%, 0.50%, 0.75%, and 1.00% by weight of cement and comparing the results with their respective standard mortars. The results allow the identification of differential trends between the two types of cement, as well as the impact of nanomaterial dosage on the reduction or increase in absorption capacity. Taking these results into account, some differences were observed between mortars with Type N and Type HS cement.

Table 5. Compressive strength results for type N mortars over time, at different percentages of nano-clay.

Age	Standard	% of nanoclay in mortar			
		0,25%	0,50%	0,75%	1%
(days)	(MPa)	(MPa)	(MPa)	(MPa)	(MPa)
1	1,06	1,21	0,81	1,21	0,95
3	4,48	4,23	3,69	4,66	4,70
7	6,83	7,14	4,88	8,44	7,63
28	10,22	12,74	9,76	9,65	10,15
90	12,60	16,61	12,94	13,16	13,81

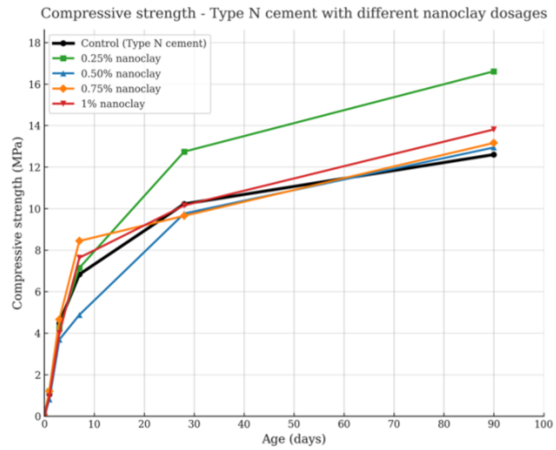

Figure 7. Compressive strength curves for type N mortar, for each percentage of nano-clay, and its behavior over time.

3.2.2. Type HS Cement

At 90 days, the standard reached 30.54 MPa and the mixture with 0.25% nanoclay reached 37.87 MPa (+24.0%). The 0.75% dosage also performed well (34.49 MPa), although it was below the optimum. Dosages of 0.50% and 1.00% did not significantly exceed the standard. The compressive strength results are presented in Table 7, and their evolution over time is shown in Figure 8.

Table 6. Compressive strength results for HS-type mortars over time, at different percentages of nano-clay.

Age	Standard	% of nanoclay in mortar			
		0,25%	0,50%	0,75%	1%
(days)	(MPa)	(MPa)	(MPa)	(MPa)	(MPa)
1	5,13	5,19	4,47	5,16	4,97
3	14,69	15,48	14,25	13,58	9,89
7	20,20	21,22	19,06	24,09	19,76
28	25,37	29,31	25,88	26,80	25,88
90	30,54	37,87	29,62	34,49	32,58

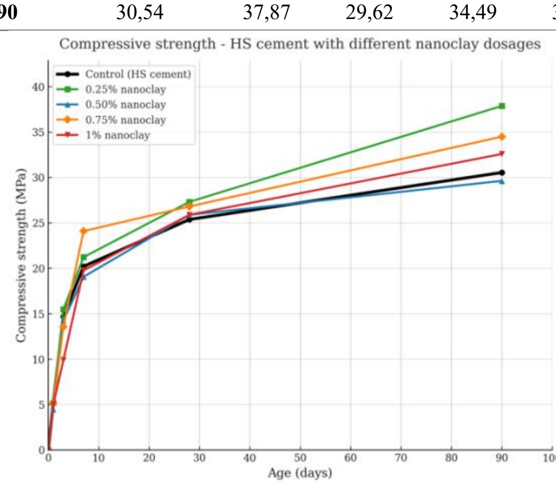

Figure 8. Compressive strength curves HS mortar, for each percentage of nano-clay, and its behavior over time

3.3.1. Type N Cement

In mortar made with Type N cement, the standard showed an average absorption of 12.00% at 28 days. The addition of 0.25% nanoclay slightly reduced the value to 11.89%, while the 0.50% dosage achieved the lowest recorded absorption (10.71%), showing a slight improvement in the compactness of the matrix. However, from 0.75% onwards, the trend was reversed, with 10.85% and 11.96% recorded at 0.75% and 1.00%, respectively, values close to those of conventional mortar. These results suggest that nanoclay can contribute to a temporary refinement of the porous network at low doses, but at higher proportions, particle agglomeration limits its positive effect. The absorption results are presented in Table 8, and their comparison according to the percentage of nanomaterial is shown in Figure 9.

Table 7. Absorption results for type N mortar

% Nanoclay	#	Dry Mass (gr)	Wet Mass (gr)	ABSORPTION	
Standard	a	253,98	284,20	11,90%	12,00%
	b	263,02	294,83	12,09%	
0,25%	a	269,46	301,27	11,81%	11,89%
	b	263,33	294,85	11,97%	
0,50%	a	268,30	298,44	11,23%	10,71%
	b	261,82	288,50	10,19%	
0,75%	a	267,09	292,09	9,36%	10,85%
	b	265,42	298,15	12,33%	
1,00%	a	259,25	289,60	11,71%	11,96%
	b	269,32	302,20	12,21%	

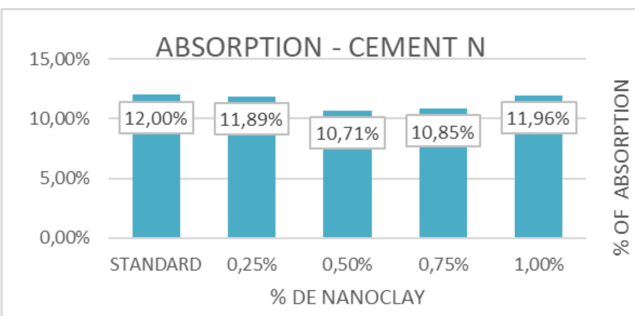

Figure 9. Comparison of the % absorption in each % of nanomaterial in type N mortar.

3.3.2. Type HS Cement

In mortar made with Type HS cement, the standard sample had an absorption rate of 10.07%. With the addition of 0.25% nanoclay, the absorption rate increased slightly to 10.29%, which could be due to initial interference in the hydration process. At 0.50%, the value remained practically the same as the standard (10.12%), with no significant changes. From 0.75% and 1.00% onwards, there was a slight reduction to 9.72% and 9.66%, respectively, suggesting a more pronounced microfilling effect at higher proportions. However, the overall variations are minimal and do not imply significant improvements in terms of durability. The absorption results are presented in Table 9, while their comparison according to the percentage of nanomaterial is shown in Figure 10.

Table 8. Absorption results for type HS mortar.

% Nanoclay	#	Dry Mass (gr)	Wet Mass (gr)	ABSORPTION	
Standard	a	258,75	284,67	10,02%	10,07%
	b	255,16	280,98	10,12%	
0,25%	a	281,32	310,06	10,22%	10,29%
	b	283,42	312,79	10,36%	
0,50%	a	273,05	300,44	10,03%	10,12%
	b	275,71	303,85	10,21%	
0,75%	a	281,17	307,39	9,33%	9,72%
	b	273,84	301,54	10,12%	
1,00%	a	282,57	309,48	9,52%	9,66%
	b	280,16	307,59	9,79%	

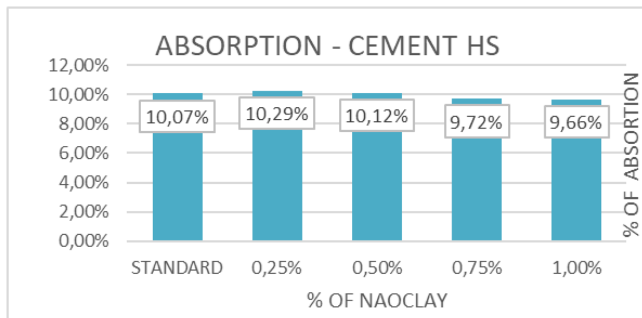

Figure 10. Comparison of the % absorption in each % of nanomaterial in HS-type mortar.

3.4. Surface Permeability

3.4.1. Type N Cement

The minimum absorption was 10.71% with 0.50% nanoclay, compared to 12.00% for the standard. However, the differences were not significant. The contact angle remained hydrophilic (<90°) in all dosages, with 0.25% showing less dispersion of values, suggesting greater surface homogeneity. The comparative permeability results obtained from the contact-angle measurements are presented in Table 10.

3.4.2. Type HS Cement

Absorption remained stable, with values between 9.66% and 10.29%. The standard mortar was hydrophobic (≈100°), but the incorporation of any amount of nanoclay reduced the angle below 90°, increasing its affinity with water. The effect was more pronounced at 0.75% and 1.00%, with values below 45°. The comparative permeability results obtained for the Type HS mortar are presented in Table 11.

Table 9. Comparison of permeability results (contact angle) between mortar with standard N-type cement and mortar with % nano-clay

PERMEABILITY – MORTAR WITH CEMENT N						
% NANOCLAY	Contact angles					
	∠ right (°)		∠ left (°)		Behavior	
Standard	35.212 55.824 55.152	48.73	30.291 58.901 55.742	48.31	θ < 90°	Hydrophilic
0.25%	45.589 44.162 39.208	42.99	45.13 53.516 50.163	49.60	θ < 90°	Hydrophilic
0.50%	46.865 39.946 36.982	41.26	47.663 39.547 40.668	42.63	θ < 90°	Hydrophilic
0.75%	38.498 40.657 60.927	46.69	41.608 35.335 57.615	44.85	θ < 90°	Hydrophilic
1%	40.025 59.261 37.752	45.68	45.537 56.444 51.401	51.13	θ < 90°	Hydrophilic

Table 10. Comparison of permeability results (contact angle) between mortar with standard HS cement and mortar with % nano-clay.

PERMEABILITY - MORTAR WITH HS CEMENT						
% NANOCLAY	Contact angles					
	∠ right (°)		∠ left (°)		Behavior	
Standard	103,507 99,951 98,952	100,80	101,9 99,32 99,03	100,07	θ > 90°	Hydrophobic
0,25%	75,700 81,136 69,731	75,52	77,53 72,47 68,59	72,86	θ < 90°	Hydrophilic
0,50%	44,301 85,061 62,235	63,87	49,28 86,27 53,56	63,04	θ < 90°	Hydrophilic
0,75%	42,469 31,161 41,362	38,33	31,86 26,44 28,35	28,88	θ < 90°	Highly hydrophilic
1%	58,174 51,68 52,395	54,08	34,21 41,86 49,7	41,92	θ < 90°	Hydrophilic

3.5. Microstructural Characterization

SEM, TEM, XRD, and EDS analyses confirmed that 0.25% nanoclay:

- Improves matrix compaction.
- Promotes the formation of C-S-H gel, identified by the peak at 16° in XRD.
- Increases Ca, Si, and Al content according to EDS, enhancing pozzolanic reactions.
- Partially reduces crystallinity, promoting denser and more stable amorphous phases.

3.5.1. Type N Cement

- **Scanning Electron Microscopy Analysis**

The addition of 0.25% nanoclay showed a more compact microstructure, with homogeneous plates and uniformly distributed dark areas associated with a higher density of heavy elements. This indicates a more closed and stable matrix. The comparison between the standard mortar and the mortar containing 0.25% nanoclay is shown in Figure 11.

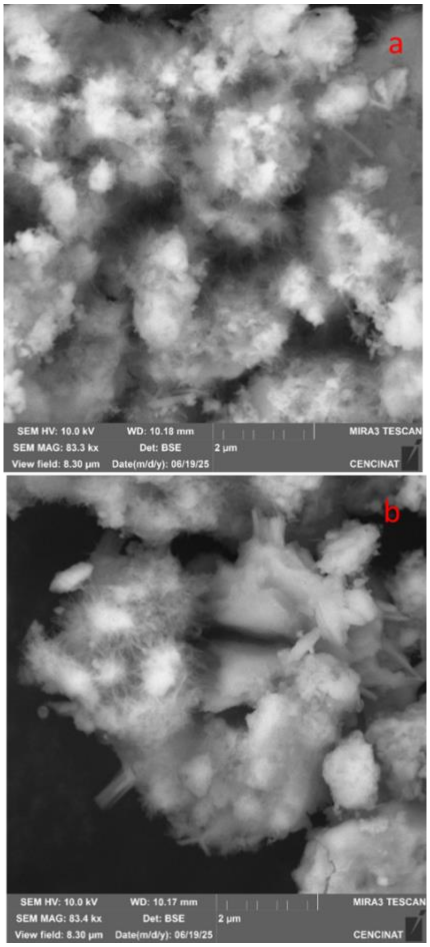

Figure 11. Comparison of SEM results between mortar with standard N-type cement (a) and mortar with 0.25% nano-clay (b).

- **Transmission Electron Microscopy Analysis**

The analysis revealed smaller, irregular particles with higher local density and dark areas, indicating intense interaction between nanoclay and hydration products. However, some agglomerations suggest that dispersion could be improved to maximize the benefits of the nanomaterial. The comparison of the TEM results is shown in Figure 12.

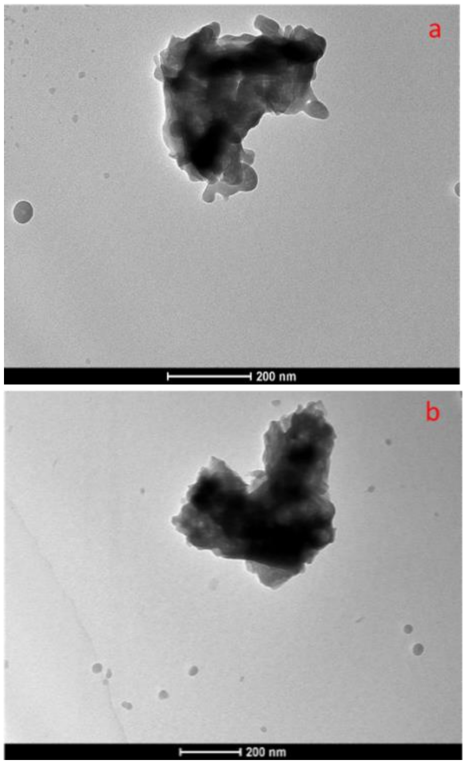

Figure 12. Comparison of TEM results between mortar with standard N-type cement (a) and mortar with 0.25% nano-clay (b).

- **X-Ray Diffraction Analysis**

The mortar with nanoclay showed a reduction in the 16° peak, indicating lower crystallinity of the C-S-H gel and favoring an amorphous structure, as well as the disappearance of the peak at 54°, associated with the consumption of secondary phases such as ettringite. The increase in the peak at 29° suggests greater portlandite formation. The XRD pattern of the standard mortar is shown in Figure 13, while the pattern corresponding to the mortar containing 0.25% nanoclay is shown in Figure 14. A comparative interpretation of the identified peaks is presented in Table 12.

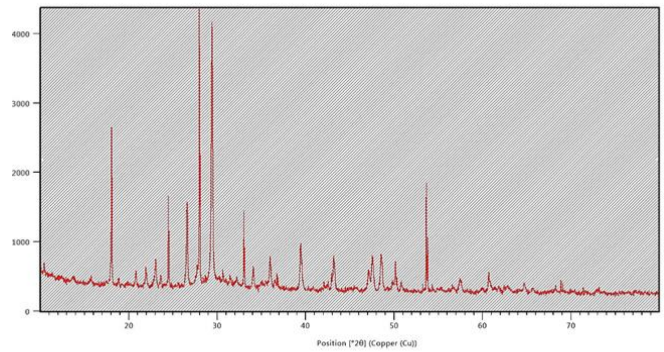

Figure 13. XRD Analysis - Type N Standard Mortar

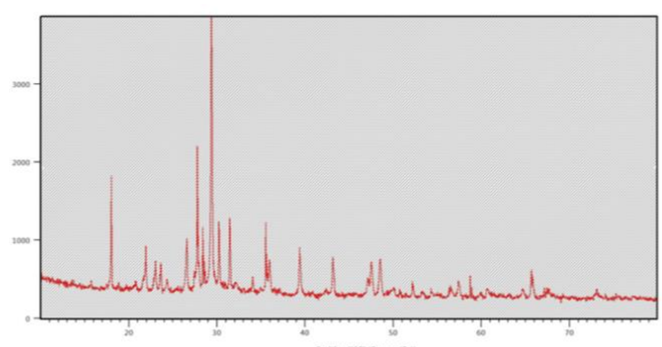

Figure 14. XRD analysis - Mortar 0.25% nanoclay - type N

Table 11. Summary of interpretation of peaks in XRD in type N mortar

ANGLE (2θ)	Possible crystalline phase	Chemical compound	Interpretation
16°	C-S-H gel not very neat	Hydrated calcium silicate	Main phase of hydrated cement, usually not very crystalline (partial amorphism).
26°	Residual silica or quartz	SiO_2 (crystalline)	It may come from mineral additives or sand.
29°	Portlandite	$Ca(OH)_2$	Direct product of the hydration of C_3S and C_2S (important for evaluating the degree of hydration).
54°	Possible ettringite or residual alite	C_3A, C_3S, or secondary phases	Disappearance may indicate consumption or transformation by the nanoclay.

- **Energy-Dispersive X-Ray Spectroscopy Analysis**

Increases in Si (+0.46%), Al (+0.26%), and Ca (+1.71%) compared with the standard confirmed the incorporation of nanoclay and its participation in pozzolanic reactions. Na appeared exclusively in the sample with nanoclay, corroborating its smectitic origin. The EDS results for the control mortar are shown in Figure 15, while those obtained for the mortar containing 0.25% nanoclay are shown in Figure 16. The comparison of the elemental composition of both samples is presented in Table 13.

3.5.2. Type HS Cement

Scanning Electron Microscopy Analysis

The standard mortar showed particles distributed in a less orderly manner. With the addition of 0.25% nanoclay, the microstructure became more compact, with homogeneous plates and a greater presence of dark areas related to denser and possibly crystallized phases. The comparison of both microstructures is shown in Figure 17.

- **Transmission Electron Microscopy Analysis**

The sample with nanoclay presented irregular particles and a more heterogeneous distribution, indicating an increase in contact surface area but lower densification if the dispersion is not optimal. The comparison of the TEM results between the standard mortar and the modified mortar is shown in Figure 18.

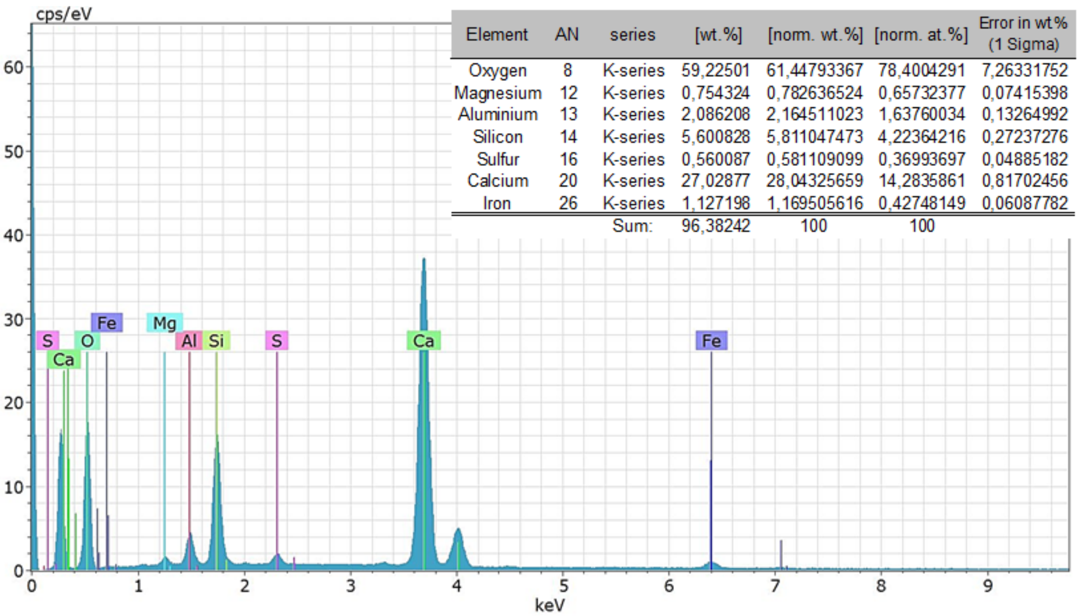

Element	AN	series	[wt.%]	[norm. wt.%]	[norm. at.%]	Error in wt.% (1 Sigma)
Oxygen	8	K-series	59,22501	61,44793367	78,4004291	7,26331752
Magnesium	12	K-series	0,754324	0,782636524	0,65732377	0,07415398
Aluminium	13	K-series	2,086208	2,164511023	1,63760034	0,13264992
Silicon	14	K-series	5,600828	5,811047473	4,22364216	0,27237276
Sulfur	16	K-series	0,560087	0,581109099	0,36993697	0,04885182
Calcium	20	K-series	27,02877	28,04325659	14,2835861	0,81702456
Iron	26	K-series	1,127198	1,169505616	0,42748149	0,06087782
		Sum:	96,38242	100	100	

Figure 15. EDS Analysis – Control Mortar – Type N.

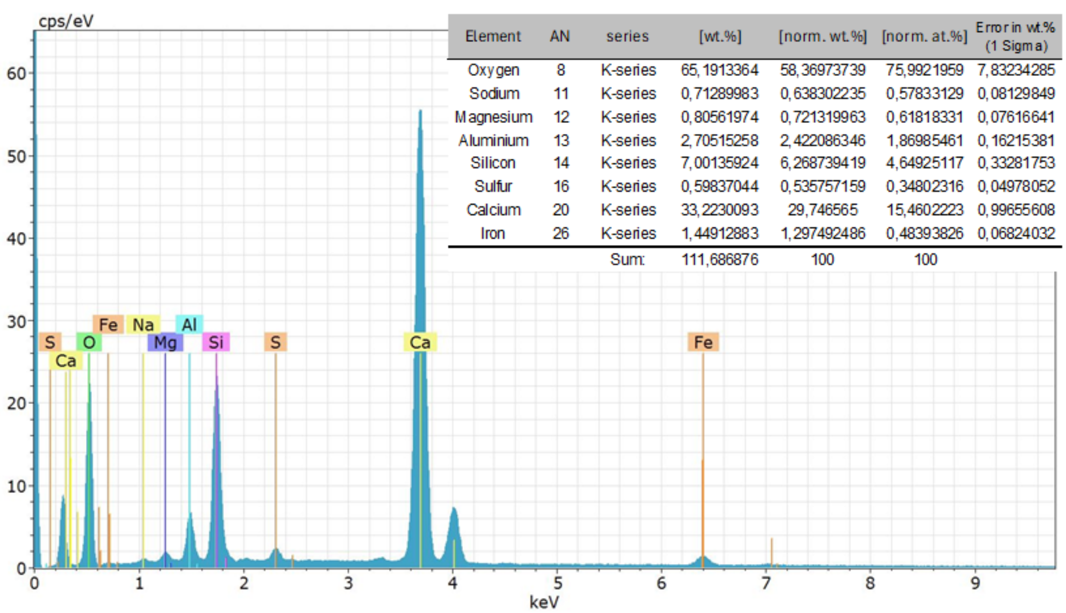

Element	AN	series	[wt.%]	[norm. wt.%]	[norm. at.%]	Error in wt.% (1 Sigma)
Oxygen	8	K-series	65,1913364	58,36973739	75,9921959	7,83234285
Sodium	11	K-series	0,71289983	0,638302235	0,57833129	0,08129849
Magnesium	12	K-series	0,80561974	0,721319963	0,61818331	0,07616641
Aluminium	13	K-series	2,70515258	2,422086346	1,86985461	0,16215381
Silicon	14	K-series	7,00135924	6,268739419	4,64925117	0,33281753
Sulfur	16	K-series	0,59837044	0,535757159	0,34802316	0,04978052
Calcium	20	K-series	33,2230093	29,746565	15,4602223	0,99655608
Iron	26	K-series	1,44912883	1,297492486	0,48393826	0,06824032
		Sum:	111,686876	100	100	

Figure 16. EDS Analysis – Mortar with 0.25% Nanoclay – Type N

Table 12. Comparison of EDS results between mortar with standard N-type (Figure 15) cement and mortar with 0.25% nano-clay (Figure 16).

Symbol	% by normalized weight 0% nanoclay	% by weight normalized 0.25% nanoclay	Variation (%)	Interpretation
O	61,45%	58,37%	▼ -3,08%	Slight decrease may be due to an increase in denser phases (such as silicates or aluminates) or partial replacement of bound water.
Na	—	0,64%	NEW Nuevo	Presence attributable to impurities in the nano-clay, as it does not appear in mortar without addition.
Mg	0,78%	0,72%	▼ -0,06%	Minor changes, probably related to the cement matrix.
Al	2,16%	2,42%	▲ +0,26%	Slight increase possibly due to the structure of the nanoclay (montmorillonite is rich in Al).
Si	5,81%	6,27%	▲ +0,46%	Increase consistent with the silica contribution of the nanoclay.
S	0,58%	0,54%	▼ -0,04%	No significant changes.
Ca	28,04%	29,75%	▲ +1,71%	Significant increase may indicate higher presence of portlandite or hydration products.
Fe	1,17%	1,30%	▲ +0,13%	It may be associated with traces of Fe in the nano-clay or cement.

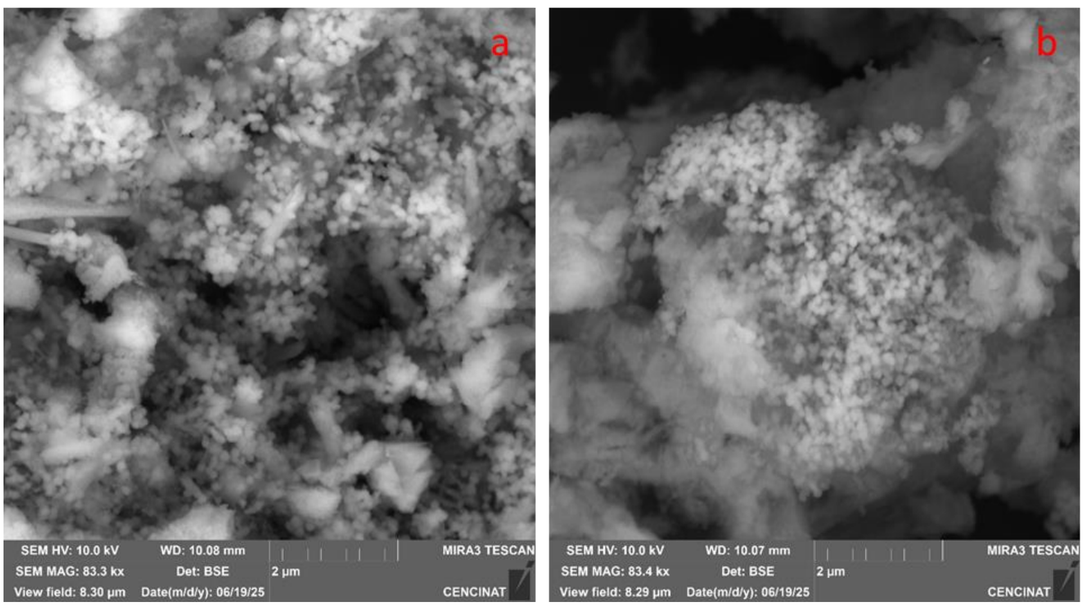

Figure 17. Comparison of SEM results between mortar with standard HS cement (a) and mortar with 0.25% nano-clay added (b).

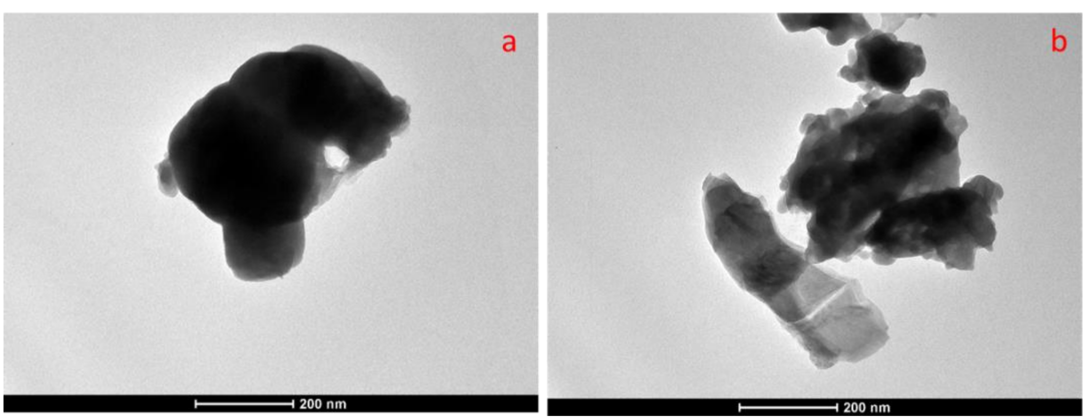

Figure 18. Comparison of TEM results between mortar with standard HS cement (a) and mortar with 0.25% nano-clay (b).

- **X-Ray Diffraction Analysis**

A decrease was observed in the intense silica peak at 26° and portlandite peak at 33°, together with the appearance of a peak at 16° associated with C-S-H gel and new peaks at 44° and 68° that could correspond to tobermorite-type phases and carbonates. This suggests greater reactivity and the formation of more complex structures. The XRD pattern of the standard mortar is shown in Figure 19, while the pattern corresponding to the mortar containing 0.25% nanoclay is shown in Figure 20. The comparative interpretation of the peaks is presented in Table 14.

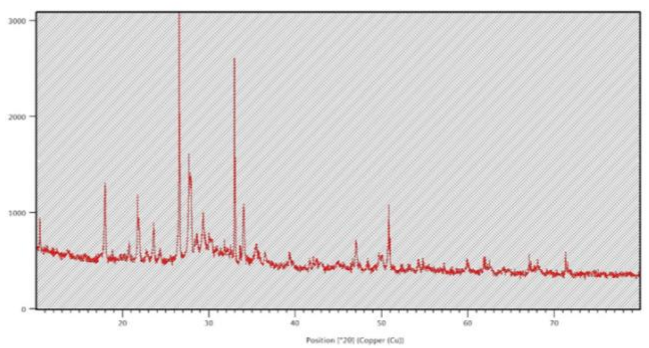

Figure 19. XRD Analysis - Standard Mortar - Type HS

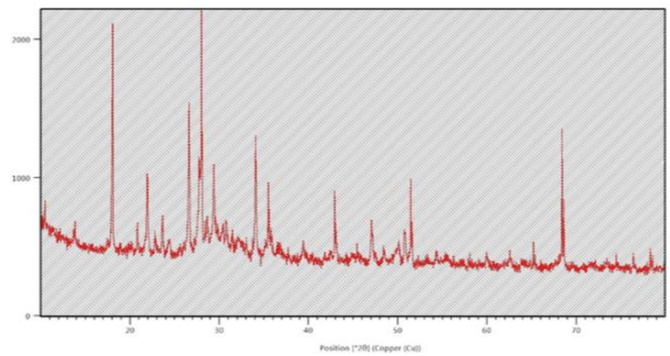

Figure 20. XRD analysis - Mortar 0.25% nanoclay - Type HS

- **Energy-Dispersive X-Ray Spectroscopy Analysis**

Slight increases in Si (+0.04%) and Ca (+2.69%), as well as the presence of Na (+0.17%), confirmed the integration of nanoclay. The reduction in Mg and Fe may be attributed to a dilution or redistribution effect. The EDS results for the control mortar are shown in Figure 21, while the results obtained for the mortar containing 0.25% nanoclay are shown in Figure 22. The comparison of the elemental composition of both samples is presented in Table 15.

Table 13. Summary of interpretation of peaks in XRD in HS-type mortar

ANGLE (2θ)	Possible crystalline phase	Chemical compound	Interpretation
16°	Hydrated calcium silicate gel	C-S-H	This peak appears only with nano-clay, indicating greater C-S-H formation, which suggests progress in hydration or an improved internal gel structure.
18°	Partially hydrated tricalcium silicate	C_3S / $C_3S{\cdot}xH_2O$	Present only without nanoclay. Its disappearance suggests that with nanoclay it has completely hydrated, transforming into C-S-H.
26°	Crystalline silica (quartz)	SiO_2	Its intensity decreases when nano-clay is added, which could be due to a reduction in free silica content or improved dissolution of quartz particles.
27°	Hydrated calcium aluminate /C-S-H	C_4AH_{13} / C-S-H	It increases with the addition of nanoclay, which may indicate that it promotes the nucleation of additional hydrated phases.
33°	Portlandite (calcium hydroxide)	$Ca(OH)_2$	Its decrease indicates that portlandite is being consumed to form secondary products (such as C-S-H), possibly favored by the presence of nanoclay.
44°	Calcite / secondary phase	$CaCO_3$ / Ca–Si–H	It appears only with nanoclay. It may be related to the formation of carbonates or secondary phases derived from pozzolanic reactions induced by nanoclay.
68°	Modified hydrated calcium silicate	C–S–H tipo Tobermorita	New peak with nanoclay. Indicates the possible development of a more ordered C-S-H gel structure in the form of tobermorite-type phases.

Table 14. Comparison of EDS results between mortar with standard HS cement (Figure 21) and mortar with 0.25% nano-clay (Figure 22).

Symbol	% by weight normalized 0% nanoclay	% by weight normalized 0.25% nanoclay	Variation (%)	Interpretation
O	56,62	55,58	-1.04 ▼	Slight reduction; possible variation in hydrated phases or structural water
Na	1,21	1,38	+0.17 ▲	Increase; confirms presence of smectite nanoclay
Mg	1,71	1,24	-0.47 ▼	Decrease; possible dilution effect or lower incorporation
Al	3,96	3,78	-0.18 ▼	Slight decrease; still high due to nano-clay
Si	9,16	9,20	+0.04 —	Slight increase; consistent with the siliceous composition of the nanomaterial
S	0,53	–	-0.53 ▼	Not detected in mortar with nanoclay
Ca	23,90	26,59	+2.69 ▲	Significant increase; greater retention of $Ca(OH)_2$ or hydrated products
Fe	2,92	2,23	-0.69 ▼	Decrease; possible phase redistribution or dilution

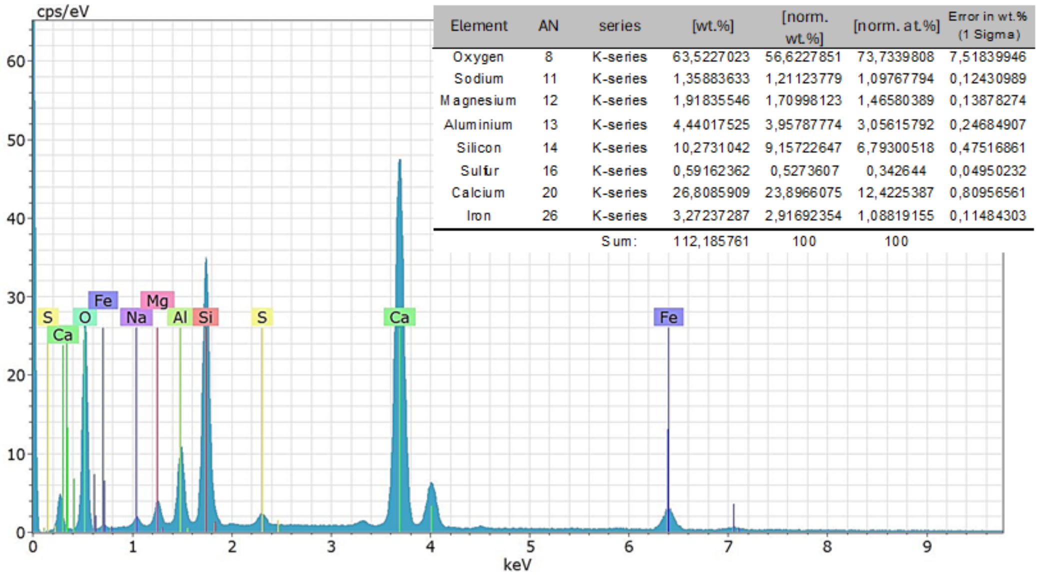

Element	AN	series	[wt.%]	[norm. wt.%]	[norm. at.%]	Error in wt.% (1 Sigma)
Oxygen	8	K-series	63,5227023	56,6227851	73,7339808	7,51839946
Sodium	11	K-series	1,35883633	1,21123779	1,09767794	0,12430989
Magnesium	12	K-series	1,91835546	1,70998123	1,46580389	0,13878274
Aluminium	13	K-series	4,44017525	3,95787774	3,05615792	0,24684907
Silicon	14	K-series	10,2731042	9,15722647	6,79300518	0,47516861
Sulfur	16	K-series	0,59162362	0,5273607	0,342644	0,04950232
Calcium	20	K-series	26,8085909	23,8966075	12,4225387	0,80956561
Iron	26	K-series	3,27237287	2,91692354	1,08819155	0,11484303
		Sum:	112,185761	100	100	

Figure 21. EDS Analysis – Control Mortar – Type HS

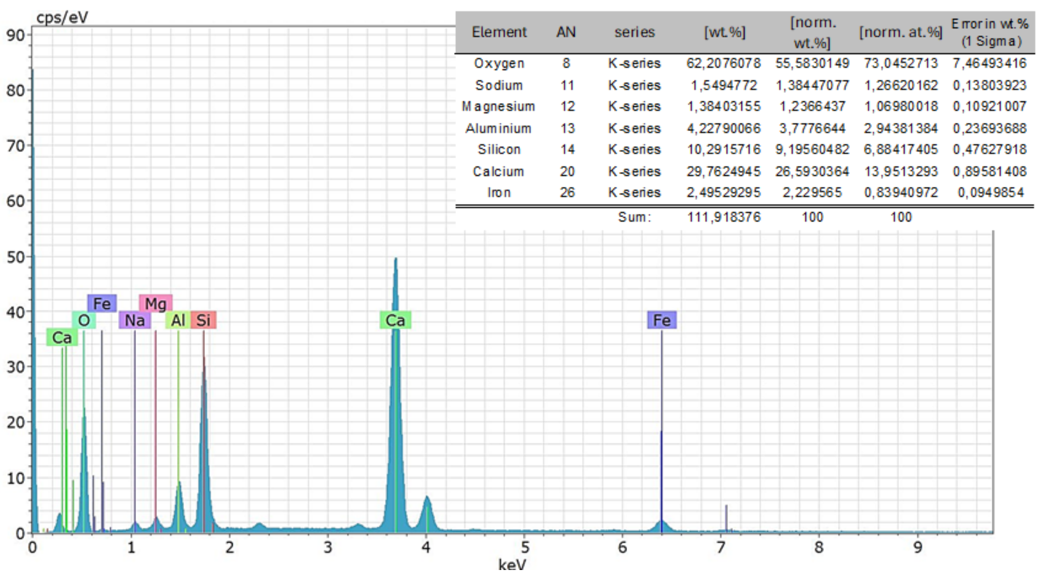

Element	AN	series	[wt.%]	[norm. wt.%]	[norm. at.%]	Error in wt.% (1 Sigma)
Oxygen	8	K-series	62,2076078	55,5830149	73,0452713	7,46493416
Sodium	11	K-series	1,5494772	1,38447077	1,26620162	0,13803923
Magnesium	12	K-series	1,38403155	1,2366437	1,06980018	0,10921007
Aluminium	13	K-series	4,22790066	3,7776644	2,94381384	0,23693688
Silicon	14	K-series	10,2915716	9,19560482	6,88417405	0,47627918
Calcium	20	K-series	29,7624945	26,5930364	13,9513293	0,89581408
Iron	26	K-series	2,49529295	2,229565	0,83940972	0,0949854
		Sum:	111,918376	100	100	

Figure 22. EDS Analysis – 0.25% Nanoclay Mortar – Type HS

3.6. Economic Analysis of Nanoclay in Mortars

The economic analysis showed that the incorporation of nanoclay in plaster mortars leads to a significant increase in the execution cost per square meter. For Type N mortar, the cost increased from 7.19 USD/m² for the conventional mix to 11.74 USD/m² for the modified mix, representing an absolute increase of 4.55 USD, of which 4.33 USD is directly attributable to the nanomaterial, dosed at 12.85 g per 0.01 m³ of mortar. Similarly, for Type HS mortar, the cost rose from 7.07 USD/m² to 11.66 USD/m², with an absolute increase of 4.59 USD, of which 4.37 USD corresponds to the nanoclay, dosed at 12.95 g per 0.01 m³ of mortar. In relative terms, these increases represent 63.26% for Type N and 64.92% for Type HS, confirming that, despite the low dosage used, the high unit cost of nanoclay has a significant impact on the final mortar price. The comparative economic results for the control and nanoclay-modified mortars are shown in Figure 23.

Figure 23. Comparative Economic Analysis: Control Mortars vs. 0.25% Nanoclay Mortars

4. Discussion

The results obtained confirm that the addition of nanoclay to plaster mortars has a significant impact on mechanical strength, but a limited effect on durability-related properties such as absorption and permeability. This duality is explained by the physical and chemical mechanisms activated by the incorporation of nanomaterials and by the characteristics of each type of cement.

- **Type N cement.**

The performance of mortar with type N cement shows that nano-clay, in low pro-portions, has a highly positive effect on mechanical strength, which is consistent with the literature on nanomaterials in cementitious matrices. The explanation lies in the fact that nano-clay acts as a nucleator for hydration products and as a filler for fine pores, generating a more compact matrix. This mechanism is supported by microstructural observations: SEM and TEM images showed a denser and more homogeneous texture, while XRD patterns showed a reduction in peaks associated with crystalline phases, confirming the transition to more stable amorphous structures.

The absorption and permeability behavior is particularly interesting, as they remained stable despite the improvement in strength. This implies that mechanical gain does not compromise durability against water ingress. In practical terms, the stability of these properties ensures that N-type mortars with nanoclay can be used in plastering applications without increasing the risk of moisture or surface deterioration. Compared to research reporting significant variations in absorption using nanosilica or nanoalumina, the results with nanoclay suggest a more localized effect, focused on mechanical densification. The importance of this sequence is clear: nanoclay improves compressive strength, reinforces microstructural homogeneity, and at the same time preserves durability stability. However, the main limitation is that the study did not evaluate pro-longed exposure to weathering cycles, where differences not yet detected could manifest themselves. Future research should focus on confirming whether this stability is maintained under real service conditions and exploring the influence of nanoclay on the adhesion of mortar to the substrate, an essential aspect in plastering.

- **Type HS cement.**

In mortar with HS cement, a positive effect of nanoclay on strength was also observed, although to a lesser extent than in N cement. This behavior can be attributed to the nature of HS cement, which already has a denser and less porous matrix, limiting the additional impact of the nanoparticles. Even so, the mechanical improvement achieved confirms that nano-clay acts as a complementary microstructural reinforcer. SEM and TEM analyses showed localized compaction of the matrix at low doses, while EDS patterns revealed a higher concentration of Ca and Si in the additive zones, suggesting greater formation of C-S-H gels.

Permeability and absorption showed equally stable behavior, with no substantial changes from the standard. This finding is significant because it confirms that, even in cement designed for aggressive environments, the addition of nanoclay does not compromise its primary function of resistance to chemical attack or increase susceptibility to water ingress. This ensures that mechanical improvements are integrated without ad-verse effects on durability. The sequence of properties in this case reinforces the consistency of the finding: strength increases, microstructure becomes denser, and at the same time, durability remains unchanged. This stability positions HS-type cement with nanoclay as a robust alternative for applications in more demanding environments. However, as with type N, a limitation of the study is the absence of long-term durability tests under field conditions, such as exposure to sulfates, moisture-dry cycles, or thermal variations.

Future research should explore the role of nanoclay in the chemical resistance of this type of cement, as well as evaluate its behavior in combination with other nanomaterials, which could further enhance its mechanical and durability properties.

- **General implications**

In both types of cement, the results converge on one key point: nano-clay significantly increases compressive strength without altering critical absorption and permeability properties. This is a key finding, as it ensures that plaster mortars can be mechanically strengthened without compromising their durability against moisture, which is highly desirable in practical applications.

This research expands the available knowledge base but also highlights the need for complementary studies that address actual service conditions and the potential for combinations with other nanomaterials. Thus, it establishes a fertile field for future research seeking to optimize mortar technology at both the structural and functional levels.

5. Results

The incorporation of nanoclay in mortars prepared with Type N and Type HS cement showed a positive effect on the development of compressive strength, particularly from the seventh day of curing. The optimal dosage was determined to be 0.25%, achieving significant increases at 90 days (16.61 MPa vs. 12.60 MPa for Type N, and 37.87 MPa vs. 30.54 MPa for Type HS). These results confirm that nanoclay, at controlled proportions, contributes to microstructural refinement, enhances the densification of the cementitious matrix, and improves long-term mechanical performance, achieving strength increases of 31.8% in Type N cement and 24.0% in Type HS cement.

Increasing the nanoclay dosage beyond 0.25% led to a decrease or plateau in strength values, attributable to dispersion issues and the formation of agglomerates that interfere with cement hydration. This highlights the importance of precise control over the amount of nanomaterial used, so that its benefits are maximized without affecting workability or the internal balance of the mix, confirming that the rational use of nano clay can be a viable strategy to improve the quality and durability of mortars.

The incorporation of nanoclay in mortars showed that a 0.25% dosage was the most suitable for both types of cement, mainly due to its stability in absorption and permeability properties. In Type N cement, the average absorption slightly de-creased from 12.00% to 11.89%, showing minimal variation. In contrast, Type HS cement exhibited a slight increase from 8.12% to 8.25%, a behavior that remains within the expected variability and can be considered stable.

Regarding the contact angle, both cements maintained a hydrophilic character without significant changes compared to the reference mix. These results allow concluding that 0.25% nanoclay does not produce marked improvements in absorption or permeability but ensures a stable and controlled behavior of these properties, indirectly favoring the mortar's durability.

The study confirms that the incorporation of 0.25% nanoclay represents the most efficient dosage in mortars prepared with Type N and Type HS cements. This proportion ensures adequate workability, maximizes compressive strength gains at 90 days, and maintains absorption and permeability properties within technically stable ranges. The observed variations in water interaction differ depending on the type of cement, demonstrating that the additive's effectiveness depends on the nature of the cementitious matrix.

The incorporation of 0.25% nanoclay in mortars with Type N and Type HS cements induces significant microstructural and chemical modifications. In Type N cement, a more compact matrix with lower porosity and better internal connectivity was observed, attributed to C-S-H gel nucleation and the integration of Si and Al with pozzolanic effect. In Type HS cement, although the microstructure was slightly less compact and somewhat heterogeneous, a greater internal contact surface was evident, promoting reactivity. These findings confirm that, despite differences in the response of each system, nanoclay acts as an effective modifier of the cementitious matrix, providing stability and potential improvements in durability.

Analyses using X-ray diffraction (XRD) and Energy Dispersive Spectroscopy (EDS) corroborate that nanoclay not only physically interacts within the mortar but also actively participates in chemical processes. The reduction of crystalline phases and the increase of amorphous phases, along with the incorporation of Na, Si, Al, and Ca, indicate a mineralogical transformation that enhances hydration and promotes the formation of secondary cementitious products. Collectively, these results validate that a controlled dosage of nanoclay favorably modifies the composition and performance of the mortar at the nanometric level, consolidating its role as a functional additive in improving physicochemical and mechanical properties.

The incorporation of 0.25% nanoclay in plaster mortars improves material performance but entails an increase in the cost per square meter. Although a small amount of nanomaterial is used, its high unit price results in a 63.26% increase in total cost compared to conventional mortar. This demonstrates that, although technically feasible, its application requires a rigorous cost–benefit evaluation before adoption in common construction projects, especially in contexts with budgetary constraints.

References

Abhilash, P. P., Nayak, D. K., Sangoju, B., Kumar, R., & Kumar, V. (2021). Effect of nano-silica in concrete: A review. Construction and Building Materials, 278, Article 122347. https://doi.org/10.1016/j.conbuildmat.2021.122347

Alvansaz, H., Hakakian, M., Alvansazyazdi, M., Salgado Reyes, N. E., & Camino Solórzano, A. M. (2019). An investigation and presentation of a model for factors influencing the agility of human resources: A case study of Yazd Electricity Distribution Company. En M. Paredes, C. Ferrás y Á. Rocha (Eds.), Information technology and systems (Vol. 918, pp. 823–834). Springer. https://doi.org/10.1007/978-3-030-11890-7_77

Alvansaz, M. F., Arévalo, B., & Arévalo, J. (2022). Adoquines de hormigón ecoamigables fabricados con la incorporación de una mezcla de micro-nano sílice. Ingenio, 5(1), 34–42. https://doi.org/10.29166/ingenio.v5i1.3784

Alvansaz Yazdi, M. F., Zakaria, R., Mustaffar, M., Abd. Majid, M. Z., Zin, R. M., Ismail, M., & Yahya, K. (2014). Bio-composite materials potential in enhancing sustainable construction. Desalination and Water Treatment, 52(19–21), 3631–3636. https://doi.org/10.1080/19443994.2013.854105

Alvansazyazdi, M., Alvarez-Rea, F., Pinto-Montoya, J., Khorami, M., Bonilla-Valladares, P. M., Debut, A., & Feizbahr, M. (2023). Evaluating the influence of hydrophobic nano-silica on cement mixtures for corrosion-resistant concrete in green building and sustainable urban development. Sustainability, 15(21), Article 15311. https://doi.org/10.3390/su152115311

Alvansazyazdi, M., Carranza Acosta, D., Sáenz Velásquez, F., & Salgado Reyes, N. E. (2025c). Sulfate attack mitigation in concrete using nanosilica and artificial intelligence: An integrated approach to structural durability. Impact Research Journal, 3(2), 109–126. https://doi.org/10.63380/irj.v3n2.2025.146

Alvansazyazdi, M., Chandi Paucar, J. E., Chávez Guamán, F. E., Bonilla-Valladares, P. M., Martial-Debut, A. P., Santamaría Carrera, J. L., Cadena Perugachi, H. A., & Logacho Morales, A. E. (2025f). Valorización del bagazo de caña de azúcar en nanosílice: Ruta optimizada para mejorar la resistencia y la sostenibilidad en morteros de cemento. Ingenio, 8(2), 95–106. https://doi.org/10.29166/ingenio.v8i2.8164

Alvansazyazdi, M., Colimba Huerta, C. A., Cando Guamán, C. E., Santamaría Carrera, J. L., Cadena Perugachi, H. A., Lascano Robalino, N. E., Bucheli García, J. A., Soledispa Pereira, E. I., Crespo Bravo, J. O., Oleas Escalante, M. F., Jiménez Merchán, C. G., Espinoza Cotera, Á. M., & Jácome Monar, E. P. (2025a). Innovación en infraestructura sostenible: Análisis avanzado de las propiedades mecánicas de adoquines permeables para una construcción resiliente y ecoeficiente. FIGEMPA: Investigación y Desarrollo, 19(1), Article e7948. https://doi.org/10.29166/revfig.v19i1.7948

Alvansazyazdi, M., Dolor Bailón, B. S., Palacios Santos, G. E., & Salgado Reyes, N. E. (2025g). Comparative review of sisal fiber and cellulose nanofiber reinforced concrete. Alpha International Journal, 3(2), 57–77. https://doi.org/10.63380/aij.v3n2.2025.142

Alvansazyazdi, M., Farinango, D., Yaucan, J., Cadena, A., Santamaría, J., Bonilla-Valladares, P. M., León, M., Debut, A., Feizbahr, M., León, L., & Ayala, B. (2024a). Exploring crack reduction in high-performance concrete: The impact of nano-silica, polypropylene, and 4D metallic fibers. International Journal of Engineering & Technology Sciences. https://www.htpub.org/article/International-Journal-Of-Engineering-And-Technology-Sciences/vol/2024/num_method/yes/articleid/1217

Alvansazyazdi, M., Figueroa, J., Paucar, A., Robles, G., Khorami, M., Bonilla-Valladares, P. M., Debut, A., & Feizbahr, M. (2024b). Nano-silica in Holcim general use cement mortars: A comparative study with traditional and prefabricated mortars. Advances in Concrete Construction, 17(3), 135–150. https://doi.org/10.12989/acc.2024.17.3.135

Alvansazyazdi, M., Flores Proaño, F. G., Reina Morales, F. X., Bonilla-Valladares, P. M., Martial-Debut, A. P., Santamaría Carrera, J. L., Cadena Perugachi, H. A., Logacho Morales, A. E., & Vélez Molina, Y. X. (2025d). Advancing sustainable construction: Analysis and evaluation of replacing Aerosil 200 nano-silica with rice husk ash nano-silica in high-strength concrete. Eídos, 18(26), 43–66. https://doi.org/10.29019/eidos.v18i26.1567

Alvansazyazdi, M., Guzmán Ruano, B. D., Noguera Benavides, C. J., Saltos Mancheno, S. D., Villalba Jácome, A. S., Reinoso Topa, J. F., Santamaría Carrera, J. L., Cadena Perugachi, H. A., & Vélez Molina, Y. X. (2025e). Revolutionizing construction materials: The role of nano-graphene in enhancing and redefining cementitious composites. Eídos, 18(26), 81–108. https://doi.org/10.29019/eidos.v18i26.1566

Alvansazyazdi, M., Logacho-Morales, A. E., Molina-Freire, W. S., Santamaría-Carrera, J. L., Cadena-Perugachi, H. A., Bonilla-Valladares, P. M., Lascano-Robalino, N. E., Bucheli-García, J. A., Soledispa-Pereira, E. I., Crespo-Bravo, J. O., Espinoza-Cotera, Á. M., Martial-Debut, A. P., Heredia-Ayala, B. G., & Tapia-Vargas, J. F. (2025j). Incorporation of nanochitin in cement mortars: An approach to enhancing durability and sustainability. FIGEMPA: Investigación y Desarrollo, 20(2), Article e7946. https://doi.org/10.29166/revfig.v20i2.7946

Alvansazyazdi, M., Moreira Alcivar, A. B., Hualpa Aldeán, W. A., & Salgado Reyes, N. E. (2025i). Durability prediction of nanoparticle-enhanced concrete using artificial intelligence: Current trends and future perspectives. Ethos Scientific Journal, 3(2), 63–78. https://doi.org/10.63380/esj.v3n2.2025.144

Alvansazyazdi, M., Sáenz Velásquez, F. F., Cedeño Cevallos, K. Y., & Salgado Reyes, N. E. (2025h). Analysis of the potential of carbon nanotubes (CNT) for carbon footprint reduction in cementitious mixtures. Kosmos: Revista Científica, 4(2), 81–104. https://doi.org/10.62943/rck.v4n2.2025.330

Alvansazyazdi, M., Salgado Reyes, N. E., Borghei, A. H., Camino Solórzano, A. M., Guzmán Rodríguez, M. S., & Rivera Valenzuela, M. A. (2019). Web-based executive dashboard reports for public works clients in construction industry. En Á. Rocha, H. Adeli, L. P. Reis y S. Costanzo (Eds.), New knowledge in information systems and technologies (Vol. 931, pp. 285–294). Springer. https://doi.org/10.1007/978-3-030-16184-2_28

Alvansazyazdi, M., Santamaría Carrera, J. L., Cadena Perugachi, H. A., Bonilla-Valladares, P. M., Martial-Debut, A. P., Heredia Ayala, B. G., Bucheli García, J. A., & Tapia Vargas, J. F. (2024d). Comparative analysis of a mortar for plastering with hydraulic cement type HS incorporating nano-iron versus cement-based mortar for masonry type N. International Journal of Engineering & Technology Sciences, Article IJETS-2405252112893. https://www.htpub.org/article/International-Journal-Of-Engineering-And-Technology-Sciences/vol/2024/num_method/yes/articleid/1220

Alvansazyazdi, M., Toala Rivera, A., Anchundia Lopez, J., & Salgado Reyes, N. E. (2025b). Application of artificial neural networks in the analysis of the influence of aluminum nanoparticles on the durability of mortar exposed to saline and humid environments. Horizon International Journal, 3(2), 86–102. https://doi.org/10.63380/hij.v3n2.2025.145

Alvansazyazdi, M., Villalba Jácome, A. S., Saltos Mancheno, S. D., Santamaría Carrera, J. L., Cadena Perugachi, H. A., León, M., León, L., Bonilla-Valladares, P. M., Heredia Ayala, B. G., Bucheli García, J. A., Martial-Debut, A. P., & Feizbahr, M. (2024c). Enhancing sustainable construction: An evaluation of nano-graphene's effectiveness in mortar composition. International Journal of Engineering & Technology Sciences, Article IJETS-2405212112892. https://www.htpub.org/article/International-Journal-Of-Engineering-And-Technology-Sciences/vol/2024/num_method/yes/articleid/1219

Alvansazyazdi, M., & Rosero, J. A. (2019). The pathway of concrete improvement via nanotechnology. Ingenio, 2(1), 3–4.

Alvansazyazdi, M., Zurita Herrera, A. J., Cedeño Aldeán, N. N., & Salgado Reyes, N. E. (2025k). Eco-friendly mortars: The role of nanoparticles and artificial intelligence in reducing the carbon footprint. Revista Ingenio Global, 4(2), 77–94. https://doi.org/10.62943/rig.v4n2.2025.331

Andrade Vieira, S. de. (2017). Análisis teórico experimental de morteros de base cemento con adición de nanopartículas [Trabajo de fin de máster, Universidad Politécnica de Madrid]. Archivo Digital UPM. https://oa.upm.es/48664/

ASTM International. (2008). ASTM D7334-08: Standard practice for surface wettability of coatings, substrates and pigments by advancing contact angle measurement. https://doi.org/10.1520/D7334-08

ASTM International. (2013). ASTM C642-13: Standard test method for density, absorption, and voids in hardened concrete. https://doi.org/10.1520/C0642-13

ASTM International. (2018). ASTM C33/C33M-18: Standard specification for concrete aggregates. https://doi.org/10.1520/C0033_C0033M-18

ASTM International. (2020a). ASTM C109/C109M-20b: Standard test method for compressive strength of hydraulic cement mortars (using 2-in. or [50-mm] cube specimens). https://doi.org/10.1520/C0109_C0109M-20B

ASTM International. (2020b). ASTM C1437-20: Standard test method for flow of hydraulic cement mortar. https://doi.org/10.1520/C1437-20

ASTM International. (2022). ASTM C1602/C1602M-22: Standard specification for mixing water used in the production of hydraulic cement concrete. https://doi.org/10.1520/C1602_C1602M-22

Bunea, G., Alexa-Stratulat, S. M., Mihai, P., & Toma, I. O. (2023). Use of clay and titanium dioxide nanoparticles in mortar and concrete—A state-of-the-art analysis. Coatings, 13(3), Article 506. https://doi.org/10.3390/coatings13030506

Cemento Selvalegre. (2024). Campeón HS granel [Ficha técnica de producto]. https://selvalegre.com.ec/productos/granel/campeon-hs/

Compañía Pétreos del Toachi. (2024). Agregados que cumplen las normas de calidad nacionales INEN y MOP y la norma internacional ASTM. https://www.copeto.com.ec/a/

Franco-Luján, V. A., Montejo-Alvaro, F., Ramírez-Arellanes, S., Cruz-Martínez, H., & Medina, D. I. (2023). Nanomaterial-reinforced Portland-cement-based materials: A review. Nanomaterials, 13(8), Article 1383. https://doi.org/10.3390/nano13081383

Gaitero Redondo, J. J. (2011). Nanotecnología en construcción: Algo más que nanopartículas. Cemento Hormigón, (942), 24–33.

Golshan, A., Rezazadeh Shirdar, M., Gohery, S., & Alvansazyazdi, M. (2012). Optimization of pre-treatment parameters before diamond coating using non-dominated sorting genetic algorithm (NSGA-II). Advanced Materials Research, 463–464, 399–405. https://doi.org/10.4028/www.scientific.net/AMR.463-464.399

Guzmán Cardona, J. M., Jaramillo Zuluaga, J. M., & Mosquera Hurtado, C. A. (2024). Efecto de la naturaleza química de nanopartículas en las propiedades mecánicas del cemento Portland. Vía Innova, 11(1), 199–216. https://doi.org/10.23850/2422068X.6821

Hernández Sampieri, R., Fernández Collado, C., & Baptista Lucio, M. del P. (2014). Metodología de la investigación (6.ª ed.). McGraw-Hill Education.

Holcim Ecuador. (2022). Cemento Holcim Maestro tipo N: Ficha técnica [Ficha técnica]. https://www.holcim.com.ec/sites/ecuador/files/2022-10/holcim-maestro_ficha-tecnica.pdf

Kafi, M. A., Sadeghi-Nik, A., Bahari, A., Sadeghi-Nik, A., & Mirshafiei, E. (2016). Microstructural characterization and mechanical properties of cementitious mortar containing montmorillonite nanoparticles. Journal of Materials in Civil Engineering, 28(12), Article 04016155. https://doi.org/10.1061/(ASCE)MT.1943-5533.0001671

López Molina, M. (2013). Nanopartículas y sus residuos: Incorporación en materiales de construcción [Trabajo de fin de máster, Universitat Politècnica de Catalunya]. UPCommons. https://hdl.handle.net/2099.1/26056

Morales, L. W., Alvansazyazdi, F., Landázuri, P., & Vásconez, W. (2020). Prevención de la contaminación por la fabricación de hormigones con nanopartículas. RISTI—Revista Ibérica de Sistemas e Tecnologias de Informação, (E30), 309–324.

Neville, A. M. (2011). Properties of concrete (5th ed.). Pearson Education.

Ray, S., Dash, J., Devi, N., Sasmal, S., & Pesala, B. (2021). Investigation of accelerated hydration in nanosilica incorporated tricalcium silicate using THz spectroscopy [Preprint]. arXiv. https://doi.org/10.48550/arXiv.2105.14482

Salgado Reyes, N., Guaña, J., Escobar, C., & Alvansazyazdi, M. (2019). Result of the methodology for learning English distance with the use of TICs: Case study, Central University of Ecuador. En Á. Rocha, L. P. Reis, H. Adeli y S. Costanzo (Eds.), New knowledge in information systems and technologies (Vol. 932, pp. 227–233). Springer. https://doi.org/10.1007/978-3-030-16187-3_22

Servicio Ecuatoriano de Normalización. (2009a). NTE INEN 156: Cemento hidráulico. Determinación de la densidad.

Servicio Ecuatoriano de Normalización. (2009b). NTE INEN 488: Cemento hidráulico. Determinación de la resistencia a la compresión de morteros en cubos de 50 mm de arista (2.ª revisión).

Servicio Ecuatoriano de Normalización. (2010a). NTE INEN 697: Áridos. Determinación del material más fino que pasa el tamiz con aberturas de 75 µm (No. 200), mediante lavado.

Servicio Ecuatoriano de Normalización. (2010b). NTE INEN 698: Áridos para hormigón. Determinación del contenido de terrones de arcilla y partículas desmenuzables.

Servicio Ecuatoriano de Normalización. (2010c). NTE INEN 855: Áridos. Determinación de impurezas orgánicas en el árido fino para hormigón.

Servicio Ecuatoriano de Normalización. (2010d). NTE INEN 856: Áridos. Determinación de la densidad, densidad relativa y absorción del árido fino.

Servicio Ecuatoriano de Normalización. (2010e). NTE INEN 858: Áridos. Determinación de la masa unitaria y el porcentaje de vacíos.

Servicio Ecuatoriano de Normalización. (2010f). NTE INEN 2518: Morteros para unidades de mampostería. Requisitos.

Servicio Ecuatoriano de Normalización. (2010g). NTE INEN 2536: Áridos para uso en morteros para mampostería. Requisitos.

Servicio Ecuatoriano de Normalización. (2011a). NTE INEN 696: Áridos. Análisis granulométrico en los áridos fino y grueso.

Servicio Ecuatoriano de Normalización. (2011b). NTE INEN 699: Áridos. Determinación de partículas livianas.

Servicio Ecuatoriano de Normalización. (2011c). NTE INEN 1806: Cementos para mampostería. Requisitos.

Servicio Ecuatoriano de Normalización. (2011d). NTE INEN 2380: Cementos hidráulicos. Requisitos de desempeño.

Servicio Ecuatoriano de Normalización. (2014). NTE INEN 2500: Cemento hidráulico. Determinación del flujo en morteros.

Sigma-Aldrich. (2011). Nanoclay, surface modified, contains 25–30 wt. % trimethyl stearyl ammonium (Product No. 682608) [Ficha de producto]. https://www.sigmaaldrich.com/ES/es/product/aldrich/682608

CRediT author statement

Alvansazyazdi, M.; Methodology, validation, formal analysis, data curation, visualization, supervision, project administration; ***Quimbia Tasgacho, D.:*** Conceptualization, formal analysis, investigation, resources, writing—original draft preparation, funding acquisition; ***Padilla Folleco, W.:*** Conceptualization, formal analysis, investigation, resources, writing—original draft preparation, funding acquisition; ***Zambrano-Roldán, K.:*** Validation, formal analysis, supervision.

All authors have read and accepted the published version of the manuscript.

Data Availability

The data supporting the findings of this study are available upon reasonable request to the corresponding author.

Conflict of interest

The authors have declared that there is no conflict of interest in this publication.

Acknowledgments: During the preparation of this manuscript/study, the author(s) used [ChatGPT5] for the purposes of [Technical Review in the English Language]. The authors have reviewed and edited the output and take full responsibility for the content of this publication.

Editor's Note

Facultad de Ingeniería Industria y Arquitectura

Revista Científica *FINIBUS* - ISSN: 2737-6451.